One-pot electronspinning of polyvinylpyrrolidone/cellulose acetate/TiO₂ nanofibrous membranes with enhanced photocatalytic properties

Jason D. Orlando, Tej B. Limbu, Basant Chitara & Fei Yan

Journal of Porous Materials

ISSN 1380-2224 Volume 27 Number 3

J Porous Mater (2020) 27:911-918 DOI 10.1007/s10934-020-00866-4



Your article is protected by copyright and all rights are held exclusively by Springer Science+Business Media, LLC, part of **Springer Nature. This e-offprint is for personal** use only and shall not be self-archived in electronic repositories. If you wish to selfarchive your article, please use the accepted manuscript version for posting on your own website. You may further deposit the accepted manuscript version in any repository, provided it is only made publicly available 12 months after official publication or later and provided acknowledgement is given to the original source of publication and a link is inserted to the published article on Springer's website. The link must be accompanied by the following text: "The final publication is available at link.springer.com".





One-pot electronspinning of polyvinylpyrrolidone/cellulose acetate/ TiO₂ nanofibrous membranes with enhanced photocatalytic properties

Jason D. Orlando¹ · Tej B. Limbu¹ · Basant Chitara¹ · Fei Yan¹

Published online: 19 February 2020

© Springer Science+Business Media, LLC, part of Springer Nature 2020

Abstract

Herein we report enhanced photocatalytic degradation of methylene blue by a novel composite material, which consists of cellulose acetate (CA), polyvinylpyrrolidone (PVP), and TiO₂ nanofibers prepared by one-pot electrospinning. This study describes a strategy for in situ synthesis of TiO₂ nanofibers within a porous two-polymer electrospun nanofiber membrane. A hybrid composite that utilizes both the absorptive properties of CA and the photocatalytic oxidative properties of TiO₂ was created. TiO₂ nanofibers were created by electrospinning a bipolymer system consisting of PVP and CA with titanium isopropoxide (TIP) in a mixture of acetic acid, acetone and N, N-dimethylacetamide. Pores were introduced by dissolving PVP to increase surface area and enhanced access to TiO₂ and CA. Small sheets of this material were able to show substantial degradation of methylene blue (10⁻⁵ M) in as little as one day. In four days, the porous membrane exhibited approximately 200% enhancement in its removal efficiency of methylene blue, as compared with the as-synthesized CA/PVP/TiO₂ and the PVP/TiO₂ nanofiber sheets. This study offers a robust method for synthesis of this two-polymer material with variable quantities of TIP and demonstrates the potential applicability of electrospun hybrid polymer/TiO₂ nanofiber composites as thin fibrous catalytic surfaces.

Keywords Electrospinning · Bipolymers · Methylene blue · Titanium dioxide · Photocatalytic degradation

1 Introduction

Water pollution has become an ever-increasing concern to the public and the scientific community. One source of it being industrial wastewater which comes from that of dyes used for finishing and dying textiles. These dyes along with other water pollutants pose an issue to the quality of drinking water and the safety of aquatic life. Water treatment methods have been successfully implemented using adsorption, microfiltration, oxidation, biological degradation, and chemical coagulation. Novel methods for treatment using sawdust for adsorption and recycled alum sludge for

Electronic supplementary material The online version of this article (https://doi.org/10.1007/s10934-020-00866-4) contains supplementary material, which is available to authorized users.

Fei Yan fyan@nccu.edu

Department of Chemistry and Biochemistry, North Carolina Central University, Durham, NC 27707, USA coagulation have been developed to reduce the cost required to treat water especially when compared to activated carbon [1, 2]. The goal of this work was to build upon this pursuit of a low-cost water filtration method. Improving upon these materials with a potentially reusable film that could combine the adsorptive properties of cellulose acetate (CA) and the photocatalytic oxidative properties of the TiO₂ on a model dye of methylene blue [3, 4].

TiO₂ is a semiconductor with known photocatalytic properties in the anatase crystal form and can generate radical oxygen species in aqueous solution under UV light. It has been used for bactericide and oxidative degradation of organic compounds [5–8]. As a result, this makes it a highly viable compound for water filtration using photocatalytic oxidation.

Electrospinning has been successfully utilized to create nanofibers of TiO₂ of tunable morphology based on solvent and electrospinning conditions in polyvinylpyrrolidone (PVP). In this method PVP is utilized as a base polymer for its solubility in alcohols, which is needed in



the solvent to generate TiO_2 in situ using a titanium alkoxide precursor [9–11].

Electrospinning is one technique that can be easily used to generate nanofibers and films or fibrous mats of them for low cost. This morphology can allow for large surface area to volume of both cellulose acetate and TiO2 to increase both adsorptive and oxidative properties of the material. Numerous polymers have been successfully electrospun producing nanoscale fibers. Each type requiring different solvent parameters for electrospinning [12]. Electrospun material has been used for a variety of purposes including anode material in ion batteries [13, 14], tissue engineering scaffolds, antimicrobial food packaging [15], wound dressing [16], air filtration [17, 18], and catalysis [19]. As a result of both the utility and the ease of synthesis it has become an attractive area of exploration to solve a variety of problems in addition to the potential for water filtration [20-23].

This work reports a one-pot synthesis of high quality PVP/CA/TiO₂ nanofibers by electrospinning, as well as a detailed guideline on various solvent conditions that are compatible with this method of synthesis. TiO₂ nanofibers were produced with the above method of utilizing PVP as a carrier polymer with titanium isopropoxide (TIP) during electrospinning. Solvent conditions were developed to carry out this electrospinning with CA to take advantage of its adsorptive properties. This resulting two-polymer scaffold allowed for the removal of PVP through dissolution introducing porous nature and increased access to the TiO₂ while keeping the polymer scaffold nature of the material. It was shown that the resulting material displayed oxidative properties far greater than that of the PVP/TiO₂ nanofibers and that of the two-polymer system prior to the dissolution of PVP in water.

2 Experimental

2.1 Materials

Methylene blue 1 wt% was purchased from Fisher Scientific, cellulose acetate, M.W. 30,000 g mol⁻¹, from Aldrich, polyvinylpyrrolidone, M.W. 1,300,000 g mol⁻¹, from Acros Organic, and titanium(IV) isopropoxide 98+% from Acros Organic. Glacial acetic acid and pesticide grade acetone were purchased from Fisher Scientific, 200 proof ethanol from Acros Organic and N, N-dimethylacetamide 99% from Acros Organic. The UV source used was 365 nm lamp from Spectroline (EN-180L), the power supply was from Gamma High Voltage Research (ES40P-20 W/DA) and the syringe pump was from KD Scientific (KDS-100).



2.2 Electrospinning of PVP/TiO₂ nanofibers

Initially PVP/TiO₂ nanofibers were produced to optimize the conditions for electrospinning and measure the parameters that affect the morphology of the fibers created. A mixture of 10 mL ethanol, 3 mL acetic acid and 0.45 g PVP were sonicated for about 1 h until homogenous. Afterwards TIP was added in quantities of 0.5 mL up to 5.0 mL and sonicated for about 30 min until the solution was mixed. A round 20 cm collection plate was covered with aluminum foil obtained from Sigma Aldrich for sample collection after electrospinning. Electrospinning was done on these samples in a 10 mL syringe with the needle tip 12 cm from the collection plate, with an electric field from these two points at 8 kV, and with a syringe pump setting of 0.5 mL h⁻¹. Additional potentials between 6 and 16 kV were tried along with varying ejection speeds of 0.2 to 1.5 mL h⁻¹. Electrospinning was allowed to continue until all 10 mL of solution were dispensed. The resulting material was carefully pulled from the collection plate for further analysis.

2.3 Electrospinning of PVP/CA/TiO₂ nanofibers

Different solution mixtures were tried in order to create a homogenous solution of PVP, CA and TIP that met the necessary conditions for electrospinning, which are outlined in Table 1. Solvents were chosen based on previous success of electrospinning one or both polymers. A solution that contained equal parts acetone, N,N-dimethylacetamide, and acetic acid was found to meet these conditions. The above solution was made with 3 mL of each solvent component and 0.2 g of both CA and PVP. The resulting mixture was sonicated for about 1 h until everything went into solution. Once a uniform solution was obtained TIP was added in amounts from 0.5 mL to 5.0 mL and sonicated for about 30 min until it was clear again. The same round 20 cm collection plate was used covered in aluminum foil for sample isolation. The resulting mixture was electrospun in a 10 mL syringe with the needle 12 cm from the collection plate, with an electric field of 16 kV, and a syringe pump setting of 0.5 mL h^{-1} . Electrospinning continued until all 10 mL of solution were dispensed. The resulting composite was removed from the aluminum foil for further analysis and experimentation.

2.4 Raman spectroscopy of TiO₂ nanofibers

 ${\rm TiO_2}$ fibers were isolated from the polymer/ ${\rm TiO_2}$ materials using a furnace manufactured by Thermo Scientific (FB1415M). As mentioned above the anatase crystal structure is preferable for catalytic activity, which must be considered when applying heat for calcination. Due to the

Table 1 Solvent parameters for the electrospinning of TiO₂ containing PVP and CA nanofibers

Solvent	PVP (g)	CA (g)	Dissolution	TIP (mL)	Dissolution	Electrospinning
Acetone	0.1	0.1	40 min	0.5	No	_
Acetic acid/acetone (1:1)	0.1	0.1	40 min	0.5	Turned solid	-
Acetic acid	0.1	0.1	50 min	0.5	No	-
Ethanol	0.1	0.1	No	-	_	-
Ethanol/acetic acid (1:1)	0.1	0.1	10 min	0.5	20 min	Small to zero yield of fibers
Ethanol/acetic acid (1:1)	0.2	0.2	20 min	0.5	20 min	Small to zero yield of fibers
Ethanol/acetic acid (1:1)	0.2	0.2	20 min	1.0	20 min	Shortly after starting solution turned solid
Ethanol/acetic acid (7:3)	0.2	0.2	No	-	_	-
Ethanol/acetic acid (6:4)	0.2	0.2	No	-	_	-
Ethanol/acetic acid (3:7)	0.2	0.2	40 min	1.0	Turned solid	-
Ethanol/acetic acid (4:6)	0.2	0.2	70 min	1.0	No	-
Acetic acid/dimethyl acetamide (1:1)	0.16	0.4	Yes*	0.5	No*	-
Acetic acid/dimethyl acetamide (2:1)	0.16	0.4	Yes*	0.5	No*	-
Acetic acid/dimethyl acetamide (3:1)	0.16	0.4	Yes*	0.5	No*	-
Acetone/dimethyl acetamide (1:1)	0.16	0.4	Yes*	0.5	Turned solid*	-
Acetone/dimethyl acetamide (2:1)	0.16	0.4	No*	-	_	-
Acetone/dimethyl acetamide (3:1)	0.16	0.4	No*	_	_	-
Acetone/acetic acid/dimethyl acetamide (1:1:1)	0.16	0.4	Yes*	0.5	30 min	Few small brittle films collected
Acetone/acetic acid/dimethyl acetamide (1:1:1)	0.2	0.2	60 min	1.0	30 min	Small brittle films collected
Acetone/acetic acid/dimethyl acetamide (1:1:1)	0.2	0.2	60 min	1.5	30 min	Small brittle films collected
Acetone/acetic acid/dimethyl acetamide (1:1:1)	0.2	0.2	60 min	2.0	30 min	Small flexible films collected
Acetone/acetic acid/dimethyl acetamide (1:1:1)	0.2	0.2	60 min	3.0	30 min	Continuous flexible films collected

Total solvent volumes were 10 mL with indicated ratios, except for all the solvents that included dimethyl acetamide which had a total solvent volume of 9 mL. Dissolution times marked with an asterisk denote dissolution statuses after one day of ultrasonication

rutile crystal structure of ${\rm TiO_2}$ being more thermodynamically favored over the anatase form the furnace was set at 600 °C to remove polymers without entirely transitioning to this phase [10, 16]. Nanofibers were placed in ceramic crucibles and allowed to calcinate for 1 h in the furnace. Raman data was taken of these isolated fibers utilizing a 532 nm laser on a LabRAM HR Raman spectrometer from Horiba Scientific. The Raman spectroscopy allowed for the confirmation of which crystal structure the ${\rm TiO_2}$ was observed under various conditions.

2.5 Scanning electron microscopy (SEM)

Nanofibers were observed under field emission scanning electron microscope (FEI Verios 460L) to measure dimensions of grown fibers under varying conditions, and surface changes due to calcination and dissolution.

2.6 Photocatalytic oxidative potency

Comparative oxidative experiments were carried out using methylene blue. A methylene blue solution of 10⁻⁵ M was utilized for these experiments. Membranes of about 1 cm² (0.5 mg) were cut from both PVP/TiO₂ films and the bipolymer composite to be used in bifurcated 100 × 15 mm petri dishes with 15 mL of the prepared methylene blue solution. Samples were prepared of the PVP/CA/TiO₂ nanofibers to allow for dissolution of the PVP prior to the experiment by placing them in 20 mL vials with 10 mL of DI water on a shaker plate (Classic C2 New Brunswick Scientific) at 100 rpm for one day. The three types of samples were then placed under two identical UV long wave 365 nm lamps for varying lengths of time along with control samples that only contained methylene blue. After which the solutions were measured for the intensity of methylene blue absorption through the utilization of



UV-vis spectroscopy (UV3100-PC by VWR) at different intervals of time.

3 Results and discussion

3.1 TiO₂ crystal structure study for PVP/TiO₂ generated fibers

Initial electrospinning experiments were carried out according to previous work to create TiO₂ containing PVP nanofibers [16]. Conditions were chosen based on previous findings and resulted in the successful creation of PVP coated TiO₂ nanofibers. One area of interest for this study was which conditions created the different TiO₂ crystal structures. TiO₂ in the anatase crystal structure is a semi-conductor with a low band gap which allows it to demonstrate the desired photocatalytic properties needed [21, 22]. The amount of TIP used, the ejection speed used for electrospinning, and the potential used for electrospinning were explored in how they relate to crystal structure formed of the TiO2. To do this the prepared samples were calcinated in a furnace to remove the PVP and leave the TiO₂ cores for further analysis. These cores were analyzed using Raman spectroscopy at 532 nm. Of these three variables, only potential displayed a relationship to the crystal structure of the TiO₂ which is illustrated in Fig. 1. At 6 kV characteristic rutile shifts of 240, 443 and

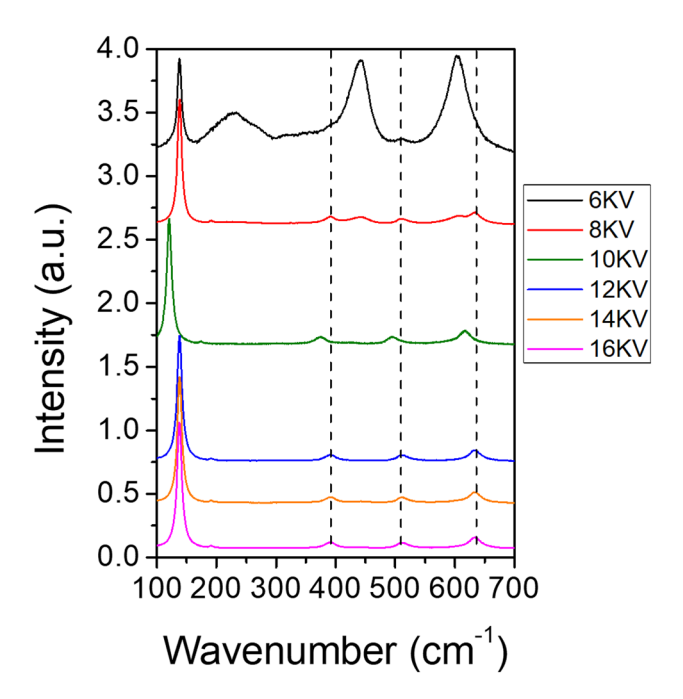


Fig. 1 Raman spectra of isolated TiO_2 made from PVP/ TiO_2 nanofibers at differing electrospinning potentials. The anatase crystal structure has characteristics shifts at 144, 394, 514, 634 cm⁻¹. The rutile crystal structure has characteristics shifts at 240, 443, 610 cm⁻¹ [24]

610 cm⁻¹ in the Raman were observed with great intensity. When the potential was at 8 kV the characteristic peaks of rutile were observed along with the characteristic peaks for the anatase at the same intensity except for the typical dominating anatase shift at 144 cm⁻¹ [24]. Above this voltage the anatase phase dominates and shifts for the rutile phase become difficult to resolve or nonexistent. The Raman spectra upwards of 8 kV show little to no difference in peaks that are present and the relative intensity and broadness of them. This data seems to suggest that there is a threshold potential for synthesizing the anatase phase of TiO₂. X-ray diffraction data (Fig. S1) obtained from the sample generated in the 16 kV electric field showed that the majority of TiO₂ exist in the anatase phase, however the rutile phase is also present [25] though decreased beyond what was detectable by Raman spectroscopy.

3.2 Development of a solvent for electrospinning both CA and PVP with TIP

A solvent that would allow for the dissolution of both PVP and CA was required for the electrospinning of this hybrid polymer. This proved challenging since PVP and CA have very different solubility characteristics. A choice made to allow for the dissolution of one polymer leaving a porous material later used for photocatalytic activity. In addition, the introduction of TIP further complicates things as far as solubility is concerned.

As seen in Table 1 there were plenty of solvent parameters that allowed for the dissolution of both polymers. However, the addition of TIP caused either the solution to turn solid or for some of the solutes, typically TiO₂ powder to settle out of the solution. This made electrospinning from this point impossible. Starting solvent parameters were chosen based upon previous experiments that had successful electrospinning of one or both polymers [16, 26, 27]. Solvent mixtures utilizing water were utilized in the literature to spin these two polymers. s was avoided due to the water sensitivity of TIP. High presence of water causes the TIP to form large TiO₂ particles and settle out of the solution. Due to this, mixtures that utilized ethanol, acetic acid, and acetone were attempted first.

A 1:1 solvent mixture of ethanol and acetic acid showed some promise being able to dissolve all the necessary components in addition to allowing some level of electrospinning. The yield of the material was small and thought maybe to be due to the small amount of each polymer used. The same conditions were repeated in a new experiment utilizing 0.2 g of each polymer as opposed to 0.1 g. This resulted in more electrospun material. However, like the first experiment it was still just a thin layer that could not be collected without creating a fine powder of the material as it was scraped from aluminum foil collector. This solution could



not be scaled up with increasing concentration of TIP to allow for a theoretically higher weight percent of ${\rm TiO_2}$ in the material. These two factors caused this solvent mixture to be abandoned in the pursuit of a solvent mixture that utilized dimethyl acetamide.

Investigation led to a 1:1:1 mixture of dimethyl acetamide, acetone and acetic acid to be used for creation of the two-polymer system. At first only small brittle films were collected even upon adjusting the ratio of the polymers knowing that experience showed PVP fibers to be quite flexible. Unlike the previous solution it was found that an increase in the amount of TIP and therefore higher wt% TiO₂ created large continuous flexible films. This trend can be seen in Fig. 2 with the increasing size of the sheets collected as TiO2 concentration increased. Increase in TiO2 concentration also resulted in a change in the physical characteristics of the isolated polymer sheets. Those films that were collected with the higher concentrations of TiO₂ made cloth like large fibrous mats. Typically allowing for the isolation of the material as just one or two continuous sheets. Whereas the low TiO₂ concentration sheets produced brittle flakes that proved difficult to collect with large surface area.

3.3 Morphology of the PVP/TiO₂ nanofibers as observed under SEM

Similarly, to the use of Raman to explore the different crystal structures formed under various electrospinning conditions. SEM was employed to observe the formed TiO₂/PVP nanofibers that were synthesized under different conditions. The samples created with varying concentrations of TIP, different ejection speeds, and different potentials used were compared. These samples were observed before and after calcination. It was discovered that changes in TiO₂ concentration affected the morphology of the nanofibers that were created. PVP/TiO2 nanofibers created with low concentrations of TiO2 exhibited beading. These fibers additionally displayed a curvier structure in the thinner non-beaded portion of the fibers. Whereas higher concentrations of TIP resulted in uniform straight fibers that exhibited little to no beading across the sample. This stark difference is illustrated in Fig. 3. Upon looking at the samples after calcination the observed morphology is still prevalent. This seems to point that the beading structures



Fig. 2 Physical appearance of nanofibrous sheets consisting of PVP, CA and TiO₂, as prepared with the same amounts of PVP and CA, with differing amounts of TIP increasing in concentration from left to right (1.0, 1.5, 2.0, 3.0, 4.0, 5.0 mL)

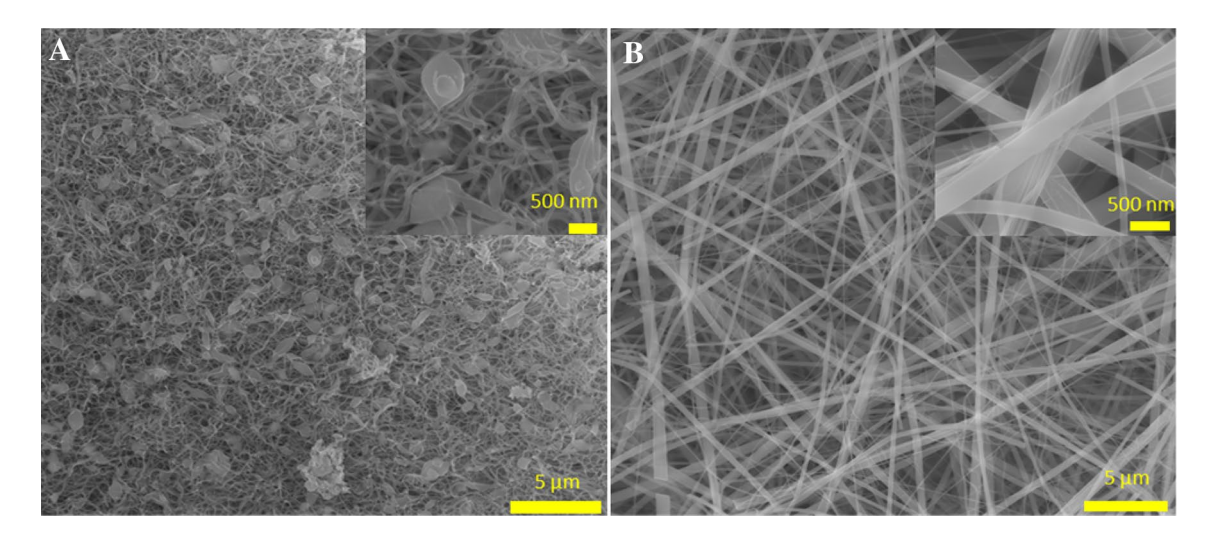


Fig. 3 SEM images of PVP/TiO₂ nanofibers that were created with 0.5 mL TIP (a) and 3.0 mL (b), showing the morphology dependence of the generated fibers on the amount of TIP



are not composed only of excess polymer as these features persist through the underlying TiO₂ fibers.

3.4 Nanofiber characteristics of the biopolymer

Raman spectra of isolated TiO₂ made from PVP/CA/TiO2 nanofibers indicate its presence in anatase structure (See Fig. S2). Just like with the PVP/TiO₂ fibers, the bipolymer fibers were observed under SEM to see if TiO₂ concentration affected their morphology as well. With the data from the PVP/TiO₂ nanofibers combined with the drastic physical differences in the bipolymer sheets grown with varying concentrations of TiO₂ some level of difference was hypothesized to be visible. Like with the PVP/TiO₂ nanofibers the two-polymer material exhibited a similar trend of beading at lower TiO₂ concentrations. In the two-polymer material beading was seen at much higher concentrations of TiO₂. In the PVP/TiO₂ nanofibers beading was no longer present in concentrations greater than 37.2 wt% TiO₂ (TIP 1.0 mL).

As seen in Fig. 4 mild beading was seen even in the samples created with 66.7 and 72.7 wt% of TiO_2 (3.0 and 4.0 mL of TIP). This trend slowly fades off until a concentration of 77.0 wt% of TiO_2 (5.0 mL TIP) was reached where beading was essentially nonexistent. As seen in Fig. 4a even at 57.2 wt% TiO_2 (2.0 mL TIP) in the two-polymer material

the sample has a similar degree of beading to that of Fig. 3a which has half the amount of TIP going into a 10 mL solution as opposed to a 9 mL one and is therefore more than twice as concentrated.

3.5 Comparative oxidation of methylene blue between PVP/CA/TiO₂ and that of the PVP/TiO₂ nanofibers

Photocatalytic oxidative degradation of methylene blue was measured between the different TiO₂ polymer nanofiber composites made. This was done using UV-Vis to measure the absorption of methylene blue over the course of different time lengths exposed to the various materials and UV light. Several samples of PVP/CA/TiO₂ were placed in individual vials of 10 mL distilled water to allow the PVP to dissolve. Porous structures could be observed within 2 hrs of being immersed in water, as evidenced by the SEM image (Fig. S3). These samples were then compared with samples of PVP/CA/TiO2 that did not have any time to dissolve their PVP, PVP/TiO₂ nanofibers, and methylene blue that as control. These samples were placed under UV lights and the UV-Vis data of the initial 10⁻⁵ M methylene blue was taken over the course of the degradation, which had an initial intensity of 0.7561. After a week all three polymer sample

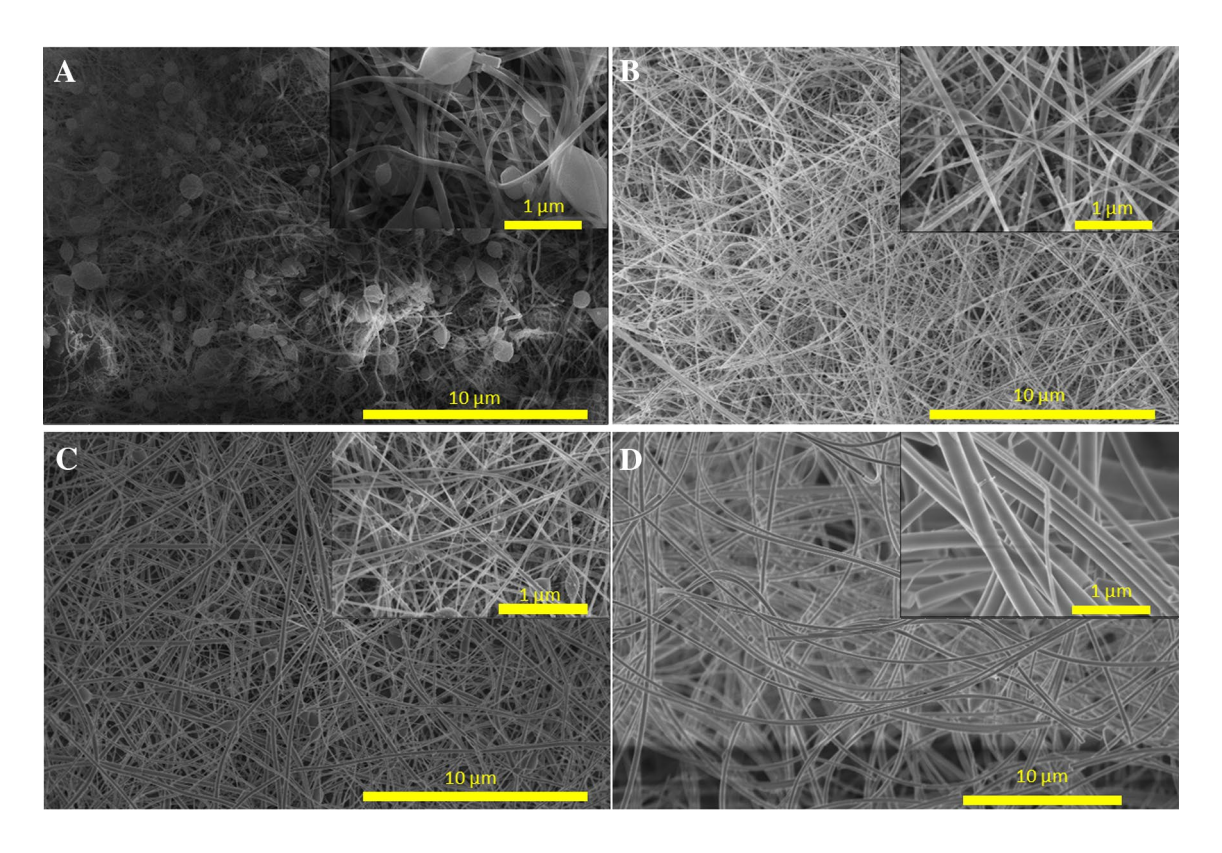


Fig. 4 SEM images of CA/PVP/TiO₂ polymers made with 2.0 mL TIP (a), 3.0 mL TIP (b), 4.0 mL TIP (c), and 5.0 mL TIP (d). The morphology of the nanofibers varies as a function of TIP concentration for electrospinning



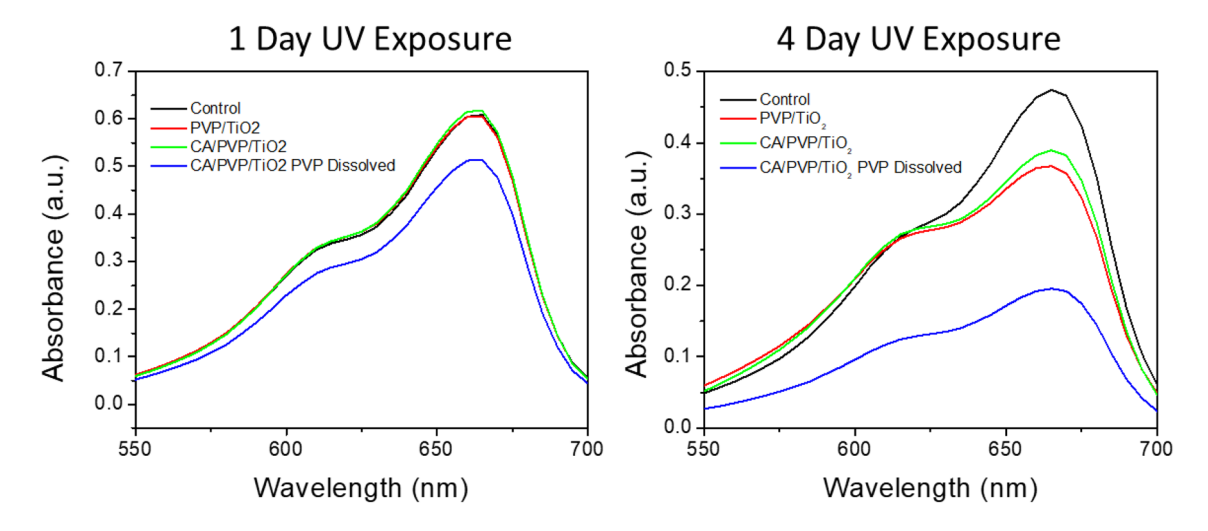


Fig. 5 The average UV-Vis spectra for the 10^{-5} M methylene blue solution with different nanofiber sheets exposed to different lengths of time of long wave UV light (365 nm)

solutions exhibited minimal UV-Vis signal for methylene blue as compared to the background (Fig. S4). However, over the course of the experiment the bipolymer material that had PVP dissolved had a much more potent reduction in absorbance.

This sample was the only one to display any type of change over the course of a day of UV exposure as compared to the control and displayed nearly twice the reduction in absorption over the course of 4 days than either of the other two materials as seen in Fig. 5. This translated to a concentration of methylene blue for the bipolymer with PVP washed of 6.8×10^{-6} M after one day and 2.59×10^{-6} M after four days. Additionally, the bipolymer turned blue over time as the experiment began, and as the solution became colorless it turned back to its original white color. This was seen at an accelerated rate with the bipolymer that had PVP dissolved and points to the discussed adsorptive properties displayed by CA. This observed property is thought to aid in the oxidation of methylene blue as it brings target analyte in contact with the material.

4 Conclusion

Novel and robust electrospinning conditions and solution parameters were developed for creating CA/PVP/TiO₂ nanofibers. This method for creating a two-polymer system displayed tunable characteristics allowing for material with higher concentrations of TIP to be synthesized. SEM characterization of both polymer fibers pointed to a threshold level of TIP that is needed in order to create uniform fibers with minimum to no beading. In the bipolymer this change in TIP used also affected the physical characteristics of the material collected along with the size of the individual sheets. Fibers

with higher concentrations of TIP were collected as large flexible fibrous sheets. By contrast the low TIP concentration material produced small brittle flakes. Fibers were observed with average diameters of less than half a micron and fibers as small as less than 100 nm. PVP/TiO₂ fibers were shown to exhibit anatase crystal structures preferentially at higher electrospinning potential.

This bipolymer structure that was created displayed oxidative characteristics even with small samples in a 10⁻⁵ M solution of methylene blue. Increased oxidative properties were observed for the two-polymer material after having the PVP dissolved as compared to the material without this dissolving time and the PVP/TiO₂ nanofibers. Additionally, this composite absorbed methylene blue over the length of the experiment turning blue, which may aid in the oxidation of lipophilic molecules as they are pulled into the composite material due to the adsorptive properties of CA. Based on the data this one-pot synthesis for the creation of this material is believed to have beneficial applications for the treatment of water, especially in poorer rural area that lack the resources for the reliable generation of potable water.

Acknowledgements The authors are grateful for the financial support of this project by the U.S. National Science Foundation (Awards # 1831133 and #1523617). This work was performed in part at the Analytical Instrumentation Facilities (AIF) at NC State University, which is supported by the state of North Carolina and the National Science Foundation (Award ECCS-1542015).

References

- 1. P. Malik, J. Hazard. Mater. 113, 81-88 (2004)
- 2. W. Chu, Water Res. **35**, 3147–3152 (2001)
- X. He, K. Male, P. Nesterenko, D. Brabazon, B. Paull, J. Luong, A.C.S. Appl, Mater. Interfaces. 5, 8796–8804 (2013)



- 4. C. Wu, J. Chern, Ind. Eng. Chem. Res. 45, 6450–6457 (2006)
- H. Yamashita, M. Harada, J. Misaka, M. Takeuchi, B. Neppolian, M. Anpo, Catal. Today 84, 191–196 (2003)
- R. Dariani, A. Esmaeili, A. Mortezaali, S. Dehghanpour, Optik 127, 7143–7154 (2016)
- P. Maness, S. Smolinski, D. Blake, Z. Huang, E. Wolfrum, W. Jacoby, Appl. Environ. Microbiol. 65, 4094–4098 (1999)
- P. Kongsong, L. Sikong, M. Masae, W. SingSang, S. Niyomwas, V. Rachpech. J. Sci. Technol. 40, 659–665 (2018)
- C. Bianca, C. Edgar, S. Pedro, A. Bernardo, C. Sandra, J. Nanotechnol. 2014, 1–5 (2014)
- Z. Tang, N. Bolong, I. Saad, J. Ayog, MATEC Web Conf. 47, 01020 (2016)
- 11. D. Li, Y. Xia, Proc. SPIE **5224**, 17–24 (2003)
- 12. J. Doshi, D. Reneker, J. Electrostat. 35, 151-160 (1995)
- J. Zhu, C. Chen, Y. Lu, Y. Ge, H. Jiang, K. Fu, X. Zhang, Carbon 94, 189–195 (2015)
- C. Chen, G. Li, Y. Lu, J. Zhu, M. Jiang, Y. Hu, L. Cao, X. Zhang, Electrochim. Acta 222, 1751–1760 (2016)
- P. Wen, D. Zhu, H. Wu, M. Zong, Y. Jing, S. Han, Food Control 59, 366–376 (2016)
- A. Ghavaminejad, A. Unnithan, A. Sasikala, M. Samarikhalaj, R. Thomas, Y. Jeong, S. Nasseri, P. Murugesan, D. Wu, C.H. Park, C. Kim, A.C.S. Appl, Mater. Interfaces. 7, 12176–12183 (2015)
- R. Zhang, C. Liu, P. Hsu, C. Zhang, N. Liu, J. Zhang, H. Lee, Y. Lu, Y. Qiu, S. Chu, Y. Cui, Nano Lett. 16, 3642–3649 (2016)

- J. Xu, C. Liu, P. Hsu, K. Liu, R. Zhang, Y. Liu, Y. Cui, Nano Lett. 16, 1270–1275 (2016)
- 19. Q. Du, J. Wu, H. Yang, ACS Catal. 4, 144–151 (2013)
- S. Tan, R. Inai, M. Kotaki, S. Ramakrishna, Polymer 46, 6128–6134 (2005)
- 21. J. Lyons, C. Li, F. Ko, Polymer 45, 7597–7603 (2004)
- 22. F. Yalcinkaya, O. Jirsak, B. Yalcinkaya, in 18th International Conference Structure and Structural Mechanics of Textiles (2011)
- O. Dosunmu, G. Chase, J. Varabhas, W. Kataphinan, D. Reneker, N.S.T.I. Nanotech, Tech. Proc. 2, 812–815 (2006)
- 24. F. Hardcastle, J. Ark. Acad. Sci. 65, 43–48 (2011)
- K. Thamaphat, P. Limsuwan, B. Ngotawornchai, J. Kasetsart, Nat. Sci. 42, 357–361 (2008)
- M. Castillo-Ortega, J. Romero-Garcã, F. Rodriguez, A. Nãjera-Luna, P. Herrera-Franco, J. Appl. Polym. Sci. 116, 1873–1878 (2010)
- 27. H. Liu, Y. Hsieh, J. Polym. Sci. B 40, 2119-2129 (2002)

Publisher's Note Springer Nature remains neutral with regard to jurisdictional claims in published maps and institutional affiliations.

